



Universiteit  
Leiden  
The Netherlands

## Synthetic tools to study ubiquitin biology

Shahul Hameed, D.A.

### Citation

Shahul Hameed, D. A. (2020, June 23). *Synthetic tools to study ubiquitin biology*. Retrieved from <https://hdl.handle.net/1887/123181>

Version: Publisher's Version

License: [Licence agreement concerning inclusion of doctoral thesis in the Institutional Repository of the University of Leiden](#)

Downloaded from: <https://hdl.handle.net/1887/123181>

**Note:** To cite this publication please use the final published version (if applicable).

Cover Page



Universiteit Leiden



The handle <http://hdl.handle.net/1887/123181> holds various files of this Leiden University dissertation.

**Author:** Shahul Hameed D.A.

**Title:** Synthetic tools to study ubiquitin biology

**Issue Date:** 2020-06-23

## Chapter 5

# Enhanced delivery of synthetic labelled ubiquitin into live cells by using next-generation Ub-TAT conjugates

**Adapted from:**

**Hameed, D.S.**, A. Sapmaz, L. Gjonaj, R. Merks, and H. Ovaa, *Enhanced Delivery of Synthetic Labelled Ubiquitin into Live Cells by Using Next-Generation Ub-TAT Conjugates*. *Chembiochem*, 2018. 19(24): p. 2553-2557.

## Summary

Proteins and macromolecules can be delivered into live cells by non-invasive techniques using cell-penetrating peptides. These peptides are easily synthesized using solid phase peptide synthesis and can be conjugated onto cargo molecules to mediate cellular delivery. We designed a TAT-based cell-penetrating ubiquitin (Ub) reagent by conjugating a dimeric disulfide-linked TAT to the C-terminus of a rhodamine-labelled Ub (RhoUb) molecule. This reagent efficiently enters the cell by endocytosis and escapes from endosomes into the cytoplasm. Once inside the cytoplasm, the delivery vehicle is proteolytically removed by endogenous deubiquitinases (DUBs) upon which the intrinsic ubiquitination machinery is able to incorporate RhoUb into ubiquitin conjugates. Our approach enables the controlled delivery of labeled or mutant Ub molecules into the cells, increasing our options for studying the ubiquitin system.

## Introduction

Ubiquitination plays an essential role in cellular protein homeostasis through regulation of protein degradation, and other key signal transduction functions. [1, 2] The 76 amino acid protein ubiquitin (Ub) modifies a targeted protein by forming covalent Ub conjugates. Its C-terminus is attached to a lysine residue or N-terminus in a target protein by the concerted action of ubiquitinating enzymes namely E1 (Ub-activating enzyme), E2 (Ub-conjugating enzyme) and E3 (Ub-ligase).[3] The process can be reversed by deubiquitinases (DUBs).[4] Ub can also form polymeric chains (PolyUb) by attaching one Ub with the N-terminal methionine or one of the seven lysine side chains to another Ub.[5] Although the ubiquitination has been extensively studied using various synthetic *in-vitro* tools,[6] there is an increasing need for tools *in vivo* to study ubiquitin conjugation in live cells.[7, 8] Therefore, the generation of methods that deliver Ub into live cells is key to further our understanding of ubiquitination in cells in real-time.

A wealth of literature describes the delivery of macromolecules into cells mediated by cell-penetrating peptides (CPPs).[9-12] A widely used CPP is the TAT peptide derived from Trans-Activator of Transcription protein of HIV-1 (TAT).[13, 14] This polycationic peptide consists of a series of lysine and arginine residues which promotes endocytosis.[15] Although TAT peptide enter cells together with its cargo molecules through the endocytic route, the escape from endosomes is essential to deliver cargo molecules into the cytoplasm and subsequently to their final destination where their functions are studied. The TAT peptides can deliver proteins into cells by simple co-incubation, but it does not guarantee efficiency in terms of collective delivery.[16] However, TAT peptide fused with proteins (TAT-fusion proteins, TFPs) provided efficient delivery into cells escaping from endosomes.[17, 18] But the endosomal escape of these TFPs was significantly impaired because of the monomeric nature of the TAT peptide fusion.[19-22] Hence, improved techniques are needed to deliver proteins that can efficiently escape from the endosomes.[23] It has been previously shown that attaching a monomeric TAT at the N-terminus of Ub resulted in endosomal entrapment of the TAT-Ub fusion protein.[24] To overcome this, Inomata *et al* has used a chemical-mediated direct translocation of a C-terminally fused Ub-TAT to deliver labelled-Ub into live cells.[25] The Ub-TAT fusion was recombinantly expressed and labelled with a dye. In order to achieve efficient delivery, a chemical mediator called 1-pyrene butyrate, along with a very high concentration of Ub-TAT fusion, was needed for direct translocation into the cytoplasm. This technique clearly indicates the potential of intracellular Ub

delivery. Recently, a disulfide-modified TAT dimer was reported to promote enhanced endosomal escape into the cytosol with no noticeable toxicity. [26, 27] Hence, we hypothesized that a Ub-TAT fusion with a dimeric disulfide-linked TAT at the C-terminus could have an enhanced endosomal escaping property to facilitate a spontaneous and efficient Ub delivery into the cytoplasm of live cells.

Our design takes advantage of Solid Phase Peptide Synthesis (SPPS) and the use of a disulfide-modified dimeric C-TAT peptide conjugated to the C-terminus of a synthetic Ub molecule. [26] We synthesized Ub with a rhodamine (Rho) tag on the N-terminus to follow the distribution using the fluorescent signal in cells. After being delivered inside the cell and escaping from the endosome, the C-TAT peptide was cleaved from RhoUb by endogenous DUBs, which allowed RhoUb to be incorporated into the ubiquitin chains by the Ub system.

## Results and discussion

RhoUb and C-TAT peptide (CKRKKRRQRRRG) precursors were synthesized by Fmoc-based solid phase peptide synthesis (Fmoc-SPPS).[28] The RhoUb-C-TAT (**1**) reagent and the C-TAT peptide were generated on a Rink amide resin in a linear fashion resulting in the amidation of the C-terminus that renders the peptides resistance to exopeptidase-degradation. We then synthesized a dimeric disulfide-linked C-TAT reagent, RhoUb-di-C-TAT (**2**) using **1** and the C-TAT peptide (Figure 1, S1). The cleavage site for DUBs is located between the Gly-Gly motif at the C-terminal end of RhoUb and the N-terminal end of the (di)-C-TAT peptide sequence (Figure 2A). The reagents **1** and **2** were refolded under non-reducing conditions before addition to cells.

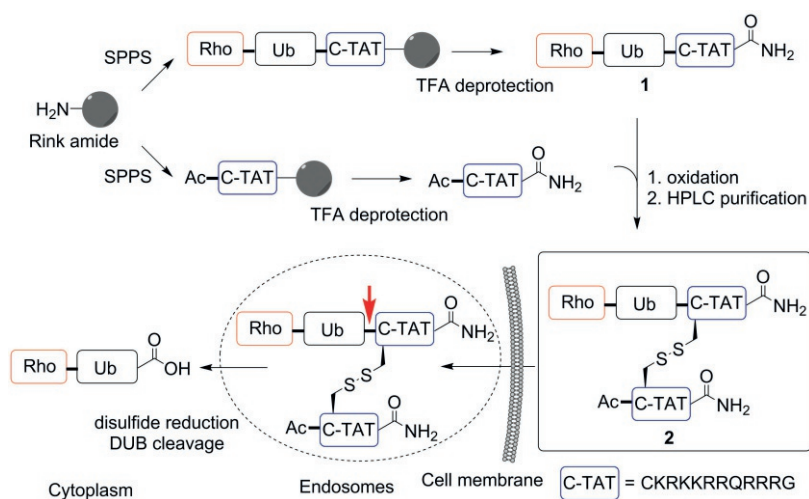


**Figure 1:** Synthesis of penetrating Rhodamine-Ub conjugates. Using Fmoc-SPPS, both the Rho-Ub-C-TAT (**1**) and C-TAT peptides were synthesized. Under oxidative conditions in PBS buffer containing 5 % DMSO, RhoUb-di-C-TAT (**2**) was generated and purified by HPLC. After **2** enters the cell by endocytosis and escapes from endosomes, DUBs cleave di-C-TAT from **2** (cleavage site is denoted by the red arrowhead) yielding RhoUb which can form Ub conjugates.

To investigate the cleavage of C-TAT fusions from RhoUb by endogenous DUBs, we performed an *in-vitro* DUB assay using cell lysate. It is known that lysate from HeLa cells contains active DUBs which were profiled using various Ub-based probes. [29] Therefore we incubated **1** and **2** with fresh HeLa cell lysate for 30 minutes at 37 °C and analysed the reaction using non-reducing SDS-PAGE (Figure 2B). We observed that the C-TAT peptide at the C-terminal end of RhoUb was cleaved from both **1** and **2** very efficiently, suggesting that free RhoUb can be released after endosomal escape into the cytoplasm to become accessible to the endogenous ubiquitin machinery.

To test the delivery of **1** and **2** into human HeLa cells, we used confocal microscopy and monitored the cellular distribution of these compounds along with the processed RhoUb derivatives. Compounds **1** and **2** were dissolved in DMSO and then refolded in PBS. HeLa cells were then incubated with compounds **1** and **2** in PBS for 5 minutes at room temperature. We avoided the use of DMEM (Dulbecco's Modified Eagle's Medium) since this medium caused disulfide reduction due to the presence of cysteine (Figure S2). The cells were then thoroughly washed with DMEM in order to reduce and remove excess of reagents from extracellular space, after which cells were fixed at different time points and studied by confocal microscopy. We showed that both **1** and **2**, but not RhoUb, were delivered inside cells after 5 minutes of incubation, implying that the reagents were cell penetrating and actively taken up by the cells due to the presence of the C-TAT fusion (Figure S3).

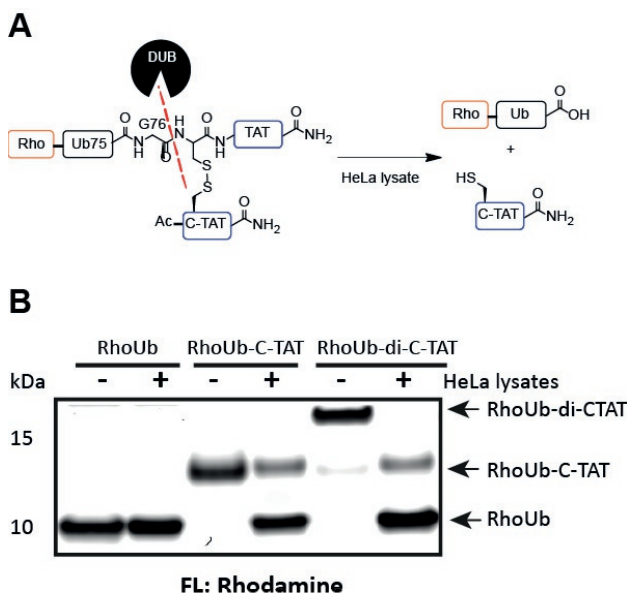


**Figure 2:** **A:** Schematic representation of DUB cleavage of RhoUb-di-C-TAT. DUBs from HeLa cell lysate cleave the peptide bond between Gly76 of RhoUb and the cysteine residue of the di-C-TAT sequence. **B:** Fluorescence scan of SDS-PAGE showing hydrolysis of C-TAT peptides from RhoUb-C-TAT conjugates before (-) and after (+) the addition of HeLa cell lysates.

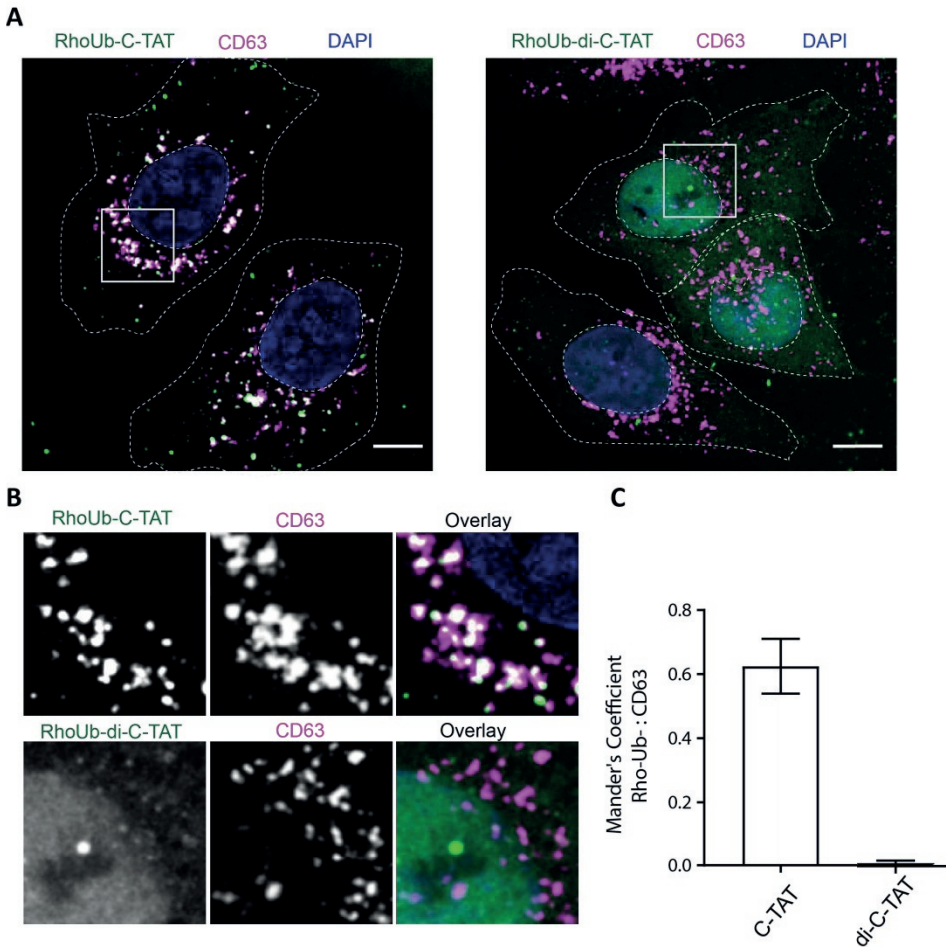


**Figure 3:** **A:** Fluorescence micrographs of HeLa cells after addition of RhoUb-cell penetrating reagents (green). Cells were incubated for 5 minutes in PBS containing different penetrating reagents and then fixed after 8 hours, stained with the anti-CD63 antibody (magenta), and DAPI (blue), and imaged by confocal microscopy. Cell boundaries and nuclei are demarcated with dashed lines. Scale bars: 10  $\mu$ m. **B:** Zoom-ins of boxed regions in (A) are shown as an overlay of RhoUb-CPP with late endosomal marker CD63. **C:** Quantification of colocalization of the different RhoUb-penetrating reagents with the late endosomal marker CD63 is shown in the graph. See also Supplementary Figure 3.

Having established that C-TAT-conjugated RhoUb reagents can be effectively taken up by the cells, we then determined whether these reagents can escape from endosomes. We introduced **1** and **2** to cells and cultured them for another 8 hours. After fixation, the cells were analyzed by confocal microscopy.

RhoUb-di-C-TAT (**2**) escaped efficiently from endosomes while RhoUb-C-TAT (**1**) almost exclusively remained in the endosomes. The RhoUb processed from **2** was predominantly localized in the nucleus as expected where it is conjugated onto histones.

*Enhanced intracellular delivery of synthetic labelled Ub-TAT conjugates*

[30] Thus the RhoUb derived from **2** behaved similarly to endogenous Ub. On the other hand, a majority of compound **1** was found only in vesicles that are positive for the late endosomal marker CD63. This implies that RhoUb-C-TAT was trapped in endosomes with no endosomal escape. (Figure 3A and B, Figure S4).

To know whether the RhoUb derived from **2** was recognized by the intrinsic Ub machinery, HeLa cells were first incubated with **1** or **2** and left for 4 hours. The cells were then exposed to MG132 which blocks proteasomal degradation of polyUb substrates resulting in the accumulation of higher order polyUb conjugates. [31] Cell lysate was prepared, and proteins were separated using SDS-PAGE followed by fluorescence scanning and blotting for the  $\beta$ -actin loading control.[32] We observed signals for higher molecular weight proteins only in cells incubated with compound **2**. We also observed an

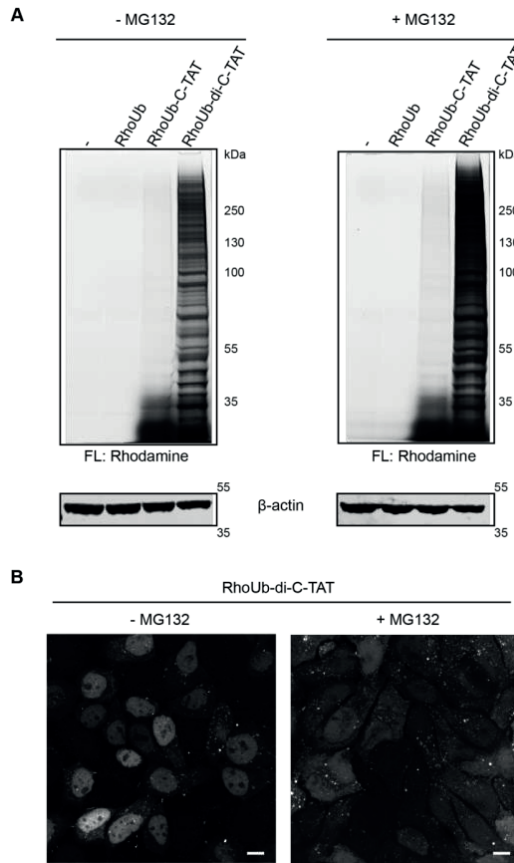


**Figure 4:** *A:* Incorporation of RhoUb in polyUb chains and higher order Ub conjugates in HeLa cells incubated with different RhoUb-penetrating reagents in the absence or presence of MG132 proteasome inhibitor. The rhodamine signal was measured using a fluorescence scanner.  $\beta$ -actin was used as a loading control. *B:* Representative fluorescence images of HeLa cells showing relocalization of RhoUb from nucleus into the cytoplasm upon treatment with 25  $\mu$ M of MG132 proteasome inhibitor. Scale bars: 10  $\mu$ m

increase in RhoUb signal for MG132 treated cells compared to non-treated cells (Figure 4A). This shows that the RhoUb processed from RhoUb-di-C-TAT reagent was dynamically re-conjugated by the ubiquitin pathway in response to MG132. Taken together, these results showed that di-C-TAT fusion compound **2** was delivered to the cytoplasm via endosomal escape and efficiently incorporated by the endogenous ubiquitin machinery.

To show the dynamics of RhoUb with respect to its nuclear and cytosolic distribution, we studied the influence of MG132 on HeLa cells treated with RhoUb-di-C-TAT. Under normal conditions, the nuclear localization is evident after the delivery of RhoUb-di-C-TAT into cells (Figure 4B, left). However, subjecting the cells to the proteasome inhibitor MG132 perturbs this pattern causing re-localization of RhoUb from nucleus to the cytoplasm (Figure 4B, right), in accordance with previous report. [30]

## Conclusions

In summary, we show that the RhoUb-di-C-TAT fusion was able to efficiently enter cells by endocytosis, escape from the endosomes into the cytoplasm and processed by endogenous DUBs to generate conjugatable RhoUb which was utilized by the intrinsic ubiquitination machinery. Thus, the presence of the C-TAT disulfide fusion proved essential for its endosomal escape.

Delivery of synthetic Ub in live cells enables studies of the ubiquitination pathway in real time. [33, 34] Here we report the design and synthesis of a simple and efficient cell penetrating Ub reagent that was spontaneously delivered inside live cells. Recently, Gui *et al* reported the use of a cell-permeable cyclic poly-Arginine-based peptide conjugated to Ub-based probes that allow DUB profiling in live cells.[35] The technique that we presented here was used in incorporating RhoUb into the intrinsic Ub machinery and may be further extended towards the delivery of Ub mutants, hydrolytically stable Ub conjugates and probes or other ubiquitin-like derivatives allowing studies of the ubiquitin system in cells in real time. [36, 37]

## Acknowledgements

We would like to thank Dris el Atmioui and Cami Talavera Ormeno for peptide synthesis; We also thank A.M.A van der Laan and L. Voortman of LUMC for microscopy facility support microscopy facility support. We would like to thank Dr. Gerbrand J. van der Heden van Noort and Dr. Koraljka Husnjak for critical reading. Work in the Ovaa lab was supported by NWO (VICI grant 724.013.002)

## References

1. Komander, D., M.J. Clague, and S. Urbe, *Breaking the chains: structure and function of the deubiquitinases*. Nat Rev Mol Cell Biol, 2009. **10**(8): p. 550-63.
2. Ciechanover, A., *The unravelling of the ubiquitin system*. Nat Rev Mol Cell Biol, 2015. **16**(5): p. 322-4.
3. Hameed, D.S., A. Sapmaz, and H. Ovaa, *How Chemical Synthesis of Ubiquitin Conjugates Helps To Understand Ubiquitin Signal Transduction*. Bioconjug Chem, 2017. **28**(3): p. 805-815.
4. Kessler, B.M., *Putting proteomics on target: activity-based profiling of ubiquitin and ubiquitin-like processing enzymes*. Expert Rev Proteomics, 2006. **3**(2): p. 213-21.
5. Akutsu, M., I. Dikic, and A. Bremm, *Ubiquitin chain diversity at a glance*. J Cell Sci, 2016. **129**(5): p. 875-80.
6. van Tilburg, G.B., A.F. Elhebshy, and H. Ovaa, *Synthetic and semi-synthetic strategies to study ubiquitin signaling*. Curr Opin Struct Biol, 2016. **38**: p. 92-101.
7. Matilainen, O., S. Jha, and C.I. Holmberg, *Fluorescent Tools for In Vivo Studies on the Ubiquitin-Proteasome System*. Methods Mol Biol, 2016. **1449**: p. 215-22.
8. Wagner, S.A., et al., *A proteome-wide, quantitative survey of in vivo ubiquitylation sites reveals widespread regulatory roles*. Mol Cell Proteomics, 2011. **10**(10): p. M111 013284.
9. Farkhani, S.M., et al., *Cell penetrating peptides: efficient vectors for delivery of nanoparticles, nanocarriers, therapeutic and diagnostic molecules*. Peptides, 2014. **57**: p. 78-94.
10. Bechara, C. and S. Sagan, *Cell-penetrating peptides: 20 years later, where do we stand?* FEBS Lett, 2013. **587**(12): p. 1693-702.
11. Copolovici, D.M., et al., *Cell-penetrating peptides: design, synthesis, and applications*. ACS Nano, 2014. **8**(3): p. 1972-94.
12. Di Pisa, M., G. Chassaing, and J.M. Swiecicki, *When cationic cell-penetrating peptides meet hydrocarbons to enhance in-cell cargo delivery*. J Pept Sci, 2015. **21**(5): p. 356-69.
13. Schwartz, J.J. and S. Zhang, *Peptide-mediated cellular delivery*. Curr Opin Mol Ther, 2000. **2**(2): p. 162-7.
14. Torchilin, V.P., *Tat peptide-mediated intracellular delivery of pharmaceutical nanocarriers*. Adv Drug Deliv Rev, 2008. **60**(4-5): p. 548-58.
15. Rudolph, C., et al., *Oligomers of the arginine-rich motif of the HIV-1 TAT protein are capable of transferring plasmid DNA into cells*. J Biol Chem, 2003. **278**(13): p. 11411-8.
16. Varkouhi, A.K., et al., *Endosomal escape pathways for delivery of biologicals*. J Control Release, 2011. **151**(3): p. 220-8.
17. Burns, K.E. and J.B. Delehanty, *Cellular delivery of doxorubicin mediated by disulfide reduction of a peptide-dendrimer bioconjugate*. Int J Pharm, 2018. **545**(1-2): p. 64-73.
18. Nischan, N., et al., *Covalent attachment of cyclic TAT peptides to GFP results in protein delivery into live cells with immediate bioavailability*. Angew Chem Int Ed Engl, 2015. **54**(6): p. 1950-3.
19. Richard, J.P., et al., *Cell-penetrating peptides. A reevaluation of the mechanism of cellular uptake*. J Biol Chem, 2003. **278**(1): p. 585-90.

20. LeCher, J.C., S.J. Nowak, and J.L. McMurry, *Breaking in and busting out: cell-penetrating peptides and the endosomal escape problem*. *Biomol Concepts*, 2017. **8**(3-4): p. 131-141.
21. Caron, N.J., S.P. Quenneville, and J.P. Tremblay, *Endosome disruption enhances the functional nuclear delivery of Tat-fusion proteins*. *Biochem Biophys Res Commun*, 2004. **319**(1): p. 12-20.
22. Gump, J.M. and S.F. Dowdy, *TAT transduction: the molecular mechanism and therapeutic prospects*. *Trends Mol Med*, 2007. **13**(10): p. 443-8.
23. Lonn, P., et al., *Enhancing Endosomal Escape for Intracellular Delivery of Macromolecular Biologic Therapeutics*. *Sci Rep*, 2016. **6**: p. 32301.
24. Loison, F., et al., *A ubiquitin-based assay for the cytosolic uptake of protein transduction domains*. *Mol Ther*, 2005. **11**(2): p. 205-14.
25. Inomata, K., et al., *High-resolution multi-dimensional NMR spectroscopy of proteins in human cells*. *Nature*, 2009. **458**(7234): p. 106-9.
26. Erazo-Oliveras, A., et al., *Protein delivery into live cells by incubation with an endosomolytic agent*. *Nat Methods*, 2014. **11**(8): p. 861-7.
27. Pescina, S., et al., *Cell penetrating peptides in ocular drug delivery: State of the art*. *J Control Release*, 2018. **284**: p. 84-102.
28. El Oualid, F., et al., *Chemical synthesis of ubiquitin, ubiquitin-based probes, and diubiquitin*. *Angew Chem Int Ed Engl*, 2010. **49**(52): p. 10149-53.
29. Leestemaker, Y., A. de Jong, and H. Ovaa, *Profiling the Activity of Deubiquitinating Enzymes Using Chemically Synthesized Ubiquitin-Based Probes*. *Methods Mol Biol*, 2017. **1491**: p. 113-130.
30. Dantuma, N.P., et al., *A dynamic ubiquitin equilibrium couples proteasomal activity to chromatin remodeling*. *J Cell Biol*, 2006. **173**(1): p. 19-26.
31. Mimnaugh, E.G., et al., *Rapid deubiquitination of nucleosomal histones in human tumor cells caused by proteasome inhibitors and stress response inducers: effects on replication, transcription, translation, and the cellular stress response*. *Biochemistry*, 1997. **36**(47): p. 14418-29.
32. Meierhofer, D., et al., *Quantitative analysis of global ubiquitination in HeLa cells by mass spectrometry*. *J Proteome Res*, 2008. **7**(10): p. 4566-76.
33. Husnjak, K. and I. Dikic, *Ubiquitin-binding proteins: decoders of ubiquitin-mediated cellular functions*. *Annu Rev Biochem*, 2012. **81**: p. 291-322.
34. Peng, J., et al., *A proteomics approach to understanding protein ubiquitination*. *Nat Biotechnol*, 2003. **21**(8): p. 921-6.
35. Gui, W., et al., *Cell-Permeable Activity-Based Ubiquitin Probes Enable Intracellular Profiling of Human Deubiquitinases*. *J Am Chem Soc*, 2018. **140**(39): p. 12424-12433.
36. Bondalapati, S., et al., *Chemical synthesis of phosphorylated ubiquitin and diubiquitin exposes positional sensitivities of e1-e2 enzymes and deubiquitinases*. *Chemistry*, 2015. **21**(20): p. 7360-4.
37. Liu, Q., et al., *A General Approach Towards Triazole-Linked Adenosine Diphosphate Ribosylated Peptides and Proteins*. *Angew Chem Int Ed Engl*, 2018. **57**(6): p. 1659-1662.

## Supplementary figures

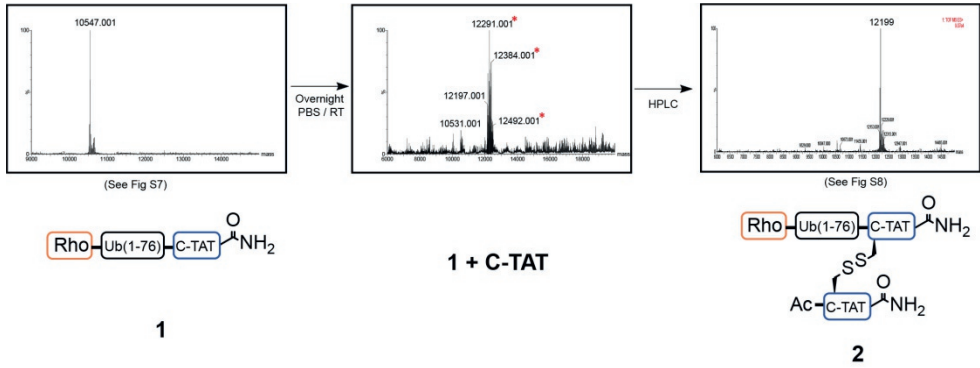


**Figure S1: Oxidation of 1 and C-TAT peptide to form 2.** RhoUb-C-TAT (1, MW: 10,547 Da), dissolved in DMSO, was added to C-TAT peptide dissolved in aerated PBS and left overnight at RT. The reaction was followed by LC/MS with measurements taken after overnight incubation showing the formation of RhoUb-di-C-TAT (2, MW: 12,199 Da). LC/MS of purified 2 is shown in figure S8. Star (\*) indicates TFA salt adducts of 2, which can be a consequence of TFA deprotection of the C-TAT peptide, commonly observed for synthetic peptides containing a high number of cationic residues in their sequence.

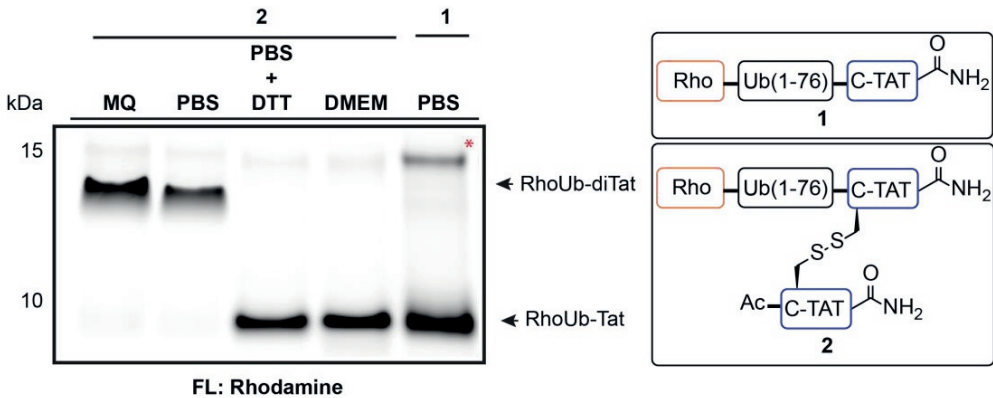


**Figure S2: Effect of DMEM in the stability of RhoUb-di-C-TAT.** RhoUb-di-C-TAT (2) was incubated in DMEM medium and in PBS containing 5 mM DTT for 30 minutes at RT and then analyzed by non-reducing SDS-PAGE. RhoUb-C-TAT (1) in PBS and 2 in MQ water were taken as controls. Star (\*) indicates an SDS-PAGE gel artefact band. Samples were resolved in a 12 % SDS-PAGE gel. The Rho signal from the gel was analyzed with a Typhoon FLA 9500.

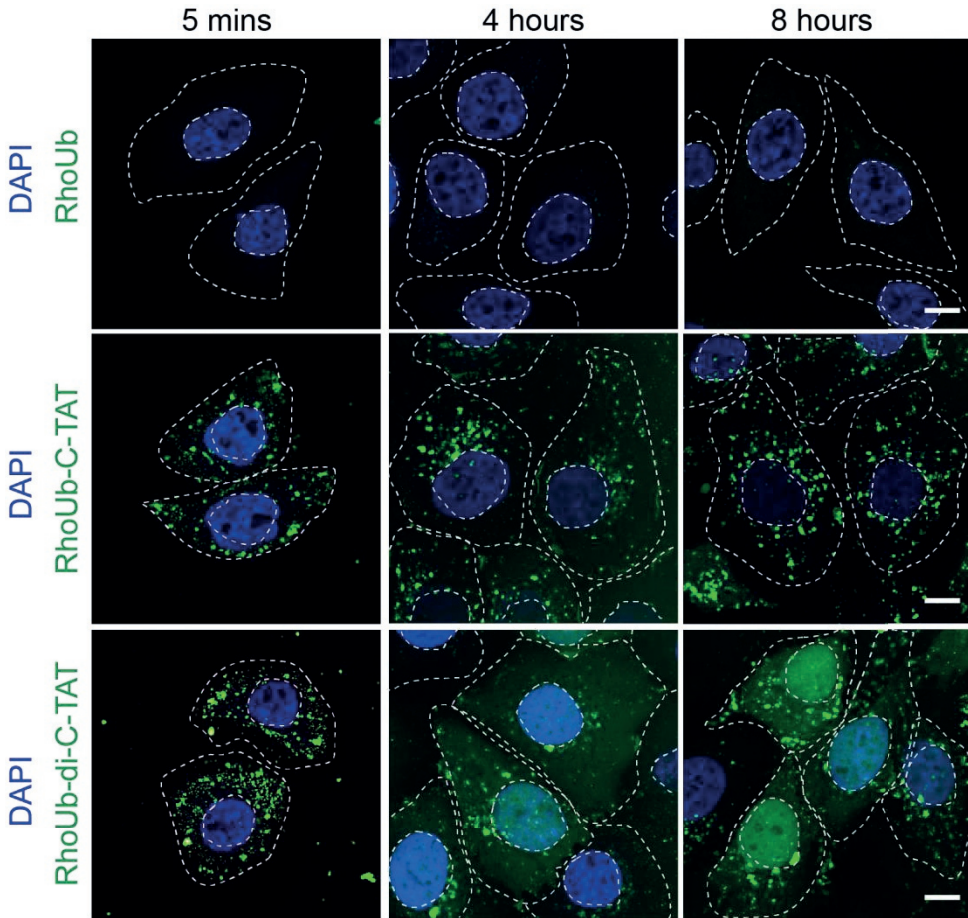


**Figure S3: Delivery of RhoUb-CPP over time.**

Confocal images of different RhoUb-CPP (green) treated HeLa cells. HeLa cells were incubated with RhoUb, RhoUb-C-TAT or RhoUb-di-C-TAT for various time intervals. Nuclear and cell boundaries are depicted in dashed lines. DAPI (blue) is a nuclear counterstain. Scale Bars: 10  $\mu$ m.

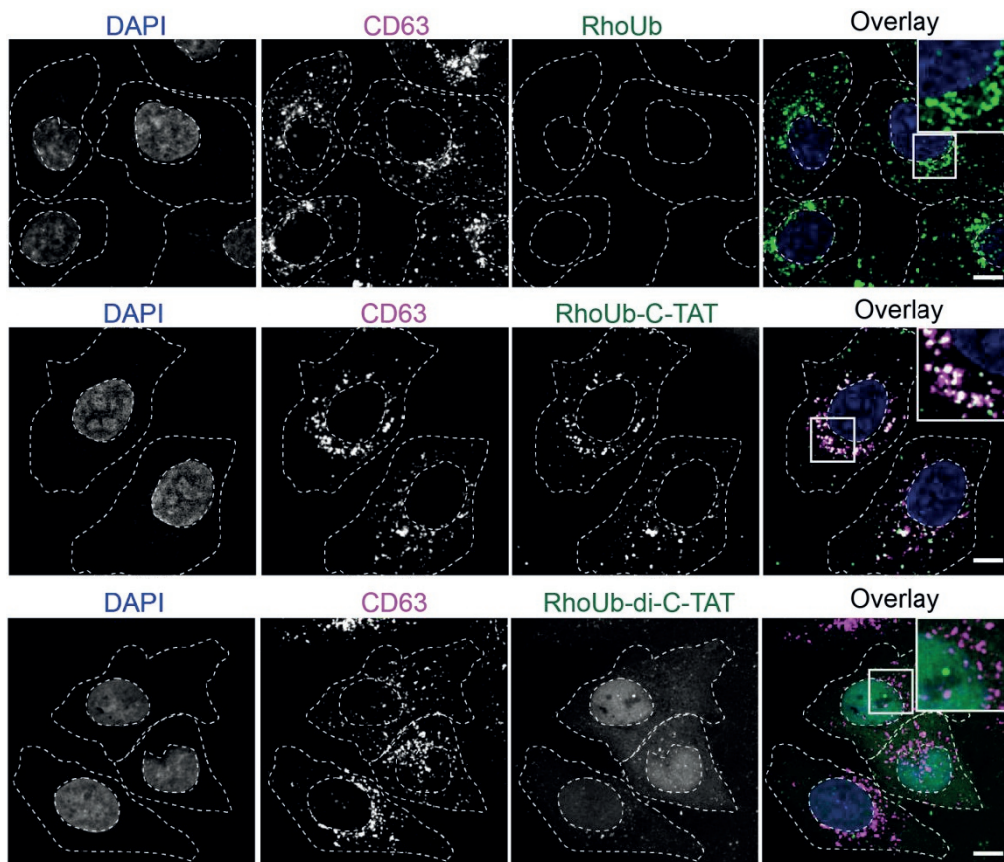


**Figure S4: Cellular localization of different RhoUb-CPP reagents.**

Confocal images of RhoUb-CPPs treated HeLa cells. Cells were incubated for 8 hours. Fixed cells were stained with a late endosomal marker, CD63, and nuclear stain, DAPI. Nuclear and cell boundaries are depicted in dashed lines. Scale bars: 10  $\mu\text{m}$ . See also Figure 3 for zoom-ins and quantification.

## Experimental section

### Synthesis of C-TAT, RhoUb, Compounds 1 and 2

**General:** All commercial materials (Aldrich, Fluka, Novabiochem) were used without further purification. All solvents were reagent grade or HPLC grade. LC/MS analysis was performed with a system containing a Waters 2795 separation module (Alliance HT), Waters 2996 Photodiode Array Detector (190–750 nm), Phenomenex Kinetex XB-C18 (2.1 x 50 mm) reversed phase column and a MicromassLCT-TOF mass spectrometer. Samples were run at 0.80 mL min<sup>-1</sup> (Kinetex C18) with the use of a gradient of two mobile phases: A) aq. formic acid (0.1 %), and B) formic acid in CH<sub>3</sub>CN (0.1 %). Data processing was performed with the aid of Waters MassLynx 4.1 software (deconvolution with Maxent1 function). Preparative HPLC was performed with a Shimadzu LC-20AD/T instrument fitted

with a Waters XBridge™ Prep C18 Column (10 x 150 mm, 5µm OBD™) with the use of gradient elution [mobile phases: A) aq. FA (0.1 %) and B) FA in CH<sub>3</sub>CN(0.1 %)].

#### **Fmoc SPPS strategy:**

SPPS was performed on a Syro II MultiSyntech Automated Peptide synthesizer using standard 9-fluorenylmethoxycarbonyl (Fmoc) based solid phase peptide chemistry at 25 µmol scales.[1] All amino acids were used in excess and dipeptides were used in positions that were determined earlier.[1] The TAT peptide containing Cysteine residue (referred as C-TAT) and Ub(1-76)-Cys-TAT (RhoUb-C-TAT) were synthesized by SPPS on H-Rink amide Chemmatrix® resin (Sigma-Aldrich) so that the C-terminal end was protected as amide. DiBoc-Rhodamine was coupled on-resin to the N-terminal end of Ub or Ub (1-76)-C-TAT compound by standard chemical coupling conditions. [2]

#### **Work-up**

The resin was dried after washing with diethyl ether under high vacuum conditions overnight. Due to the presence of Cys-tBu in the peptide sequence, we used a deprotection mix consisting of TFA/H<sub>2</sub>O/dioxane-1, 8-octane-dithiol/iPr<sub>3</sub>SiH 92.5/2.5/2.5/2.5 v/v/v/v and treated the resin with this mix for 3 hours at RT. The deprotected peptides were filtered and collected in ice-cold diethyl-ether/n-pentane 3:1 v/v mix. The resulting precipitate was then washed 3x with diethyl-ether and dried completely in air. The pellet was then dissolved in a mixture of H<sub>2</sub>O/CH<sub>3</sub>CN/HOAc (65/25/10 v/v/v) and lyophilized.

#### **Purification of the C-TAT peptide**

Due to the presence of a series of lysine and arginine residues in the TAT sequence, the synthesized C-TAT peptide was highly hydrophilic. This made purification by reversed phase HPLC more difficult as the peptide was not retained by the column. In addition, we observed at least four species of TFA-salt adducts of our C-TAT peptide (Figure S6) due to the use of TFA-mix to deprotect the peptide from SPPS. However, the purity of the synthesized C-TAT peptide was good enough to be used in the formation of compound 2 (Figure S6). Hence the C-TAT peptide was used directly after being obtained from SPPS. The C-TAT peptide was stored under an inert atmosphere as a lyophilized powder at -20 °C for future use.

#### **Synthesis of compound 2**

PBS was aerated in air for 15 minutes before being used for inter-molecular disulfide formations of the TAT peptides. Compound 1 (MW: 10,547 Da) was dissolved in DMSO at a concentration of 10 mg/mL. TAT peptide (MW: 1,625 Da) was dissolved in aerated PBS at a concentration of 4 mM. Compound 1 was added to this mix and left overnight at RT. The reaction was followed by LC/MS and the reaction was stopped after more than 90% of the desired product 2 (MW: 12,199 Da) was formed (Figure S1). The reaction was stopped by acidifying the reaction mix by adding a few drops of 10 % Formic acid.

#### **Purification of RhoUb-C-TAT and RhoUb-di-C-TAT by reverse phase HPLC**

RhoUb-C-TAT was first dissolved in DMSO. This solution was slowly added to MQ water containing 1% Formic acid and filtered through a GfxO/0.45 µm GHP membrane Acrodisc® Premium 25mm syringe filter. In the case of RhoUb-di-C-TAT, the reaction mix was first acidified adding a few drops of 10% formic acid. Later on, the reaction mix was diluted 10 times in MQ water. In both the cases, the sample was then injected onto a Waters XBridge™

### *Enhanced intracellular delivery of synthetic labelled Ub-TAT conjugates*

Prep C18 Column (10 x 150 mm, 5 $\mu$ m OBD™) at a flow rate of 10 ml/min using a preparative HPLC system mentioned in the general experimental section. The protein was purified with the gradient outlined in the following table using aq. 0.1% FA (Solvent A) and acetonitrile containing 0.1% FA (Solvent B) as eluents.

Time (in mins)	Solvent B (%)
0 $\Rightarrow$ 5	5
5 $\Rightarrow$ 7	5 $\Rightarrow$ 25
7 $\Rightarrow$ 22	25 $\Rightarrow$ 55
22 $\Rightarrow$ 24	55 $\Rightarrow$ 95
24 $\Rightarrow$ 27	95
27 $\Rightarrow$ 27.5	95 $\Rightarrow$ 5
27.5 $\Rightarrow$ 30	5

The retention time for the RhoUb-C-TAT was 10 minutes in the preparative HPLC. In the case of RhoUb-di-C-TAT, the C-TAT peptide first eluted along with the injection peak, followed by RhoUb-di-C-TAT that eluted at 12 minutes. All fractions containing the protein were confirmed by checking the mass using a LC/MS R<sub>t</sub> 3 min; Phenomenex Kinetex™ XB-C18 100A (50 x 2 x 10 mm, 2.6  $\mu$ m); solvents - MQ water with 0.1% formic acid (Solvent A) and acetonitrile containing 0.1% formic acid (Solvent B), flow rate = 0.5 mL/min, run time = 6 min, column T = 45°C. Gradient: 5%  $\Rightarrow$  95% B over 3.5 min. All samples containing pure protein were pooled together and lyophilized.

### **LC/MS analysis of the purified reagents**

All purified proteins were confirmed by checking the mass using LC/MS. Phenomenex Kinetex™ C18 (100A, 100 x 21 mm, 2.6  $\mu$ m); solvents – aq. 0.1% formic acid (Solvent A) and acetonitrile containing 0.1% formic acid (Solvent B), flow rate = 0.4 mL/min, runtime = 13 min, column T = 45°C. Gradient: 5%  $\Rightarrow$  95% B over 7.6 min. For C-TAT peptide analysis, the program used has the following parameters: flow rate = 0.5 mL/min, run time = 6 min, column T = 45°C. Gradient: 5%  $\Rightarrow$  95% B over 3.5 min.

### **Cell culture**

Human HeLa cells were cultured in DMEM (Gibco) supplemented with 7.5 % fetal calf serum (FCS, Greiner). Cells were cultured at 37°C and 5 % CO<sub>2</sub>.

### **Delivery of Ubiquitin-cell penetrating conjugates in cells**

40 x 10<sup>5</sup> Human HeLa cells were seeded into 24 well plates and grown at 37 °C and 5% CO<sub>2</sub> overnight. Compounds **1** and **2** were first dissolved in DMSO at a concentration of 1 mM. This DMSO stock was diluted into sterile PBS solution at a final concentration of 5  $\mu$ M. Different RhoUb-CPP in PBS were added to cells prepared one day before. Cells were incubated with RhoUb-CPP reagents for 5 minutes before being washed 2 times with DMEM. After this, cells were left to recover over the duration of the experiment. Cells were prepared for confocal microscopy analysis as indicated below.

### **Confocal microscopy**

For fluorescence confocal microscopy of fixed samples, cells were seeded into 24 well plates containing 13 mm slide, fixed with 3.7 % formaldehyde (acid-free, Merck Millipore) in PBS for 20 min and washed three times with PBS. Fixed cells were permeabilized with 0.1% TritonX-100 (T8787, Sigma-Aldrich) in PBS for 10 min and washed quickly twice with PBS.

After permeabilization, cells were blocked with 5% (w/v) milk powder (skim milk powder, LP0031, Oxiod) in PBS for 30 min and stained using mouse anti-CD63 antibody (NKI-C3) [3] diluted (1:100) in blocking buffer for 1 hr at room temperature. Following washes in PBS (3 x 5 min), cells were incubated in appropriate secondary anti-rabbit/mouse/rat Alexa-dye coupled antibodies (Invitrogen) diluted (1:300) in blocking buffer for 30 min. After washing (3 times 5 min), cells were mounted using ProLong Gold antifade Mounting medium with DAPI (Life Technologies, Cat# P36941). Samples were imaged using Leica SP8 microscopes equipped with appropriate solid-state lasers.

For all confocal imaging, HCX PL 63x 1.32 oil objectives and HyD detectors were used. Digital zoom ranging from 1.5x-3x was employed as applicable. Z-stacks were imaged with a z-step size of 0.5  $\mu\text{m}$  and visualized as max z-projections.

### **Ubiquitination assay**

Human HeLa cells were grown up to 70-80% confluency. The DMEM medium was removed and cells were washed with PBS. RhoUb-C-TAT and RhoUb-di-C-TAT were dissolved in PBS and added to the cells and left incubating at RT for 5 minutes. After this, the excess of RhoUb-CPPs was removed and the cells were washed twice with DMEM medium before left to incubate in DMEM for the duration of the experiment. MG132 was added to cells after 4 hours. Cells were collected after 6 hours or 8 hours in total and then lysed with lysis buffer. The samples were run by SDS-PAGE and the fluorescence signal was analyzed by Typhoon FLA 9500.

### **SDS-PAGE and western blotting**

Samples were separated by 4 – 12 % SDS-PAGE (NuPAGE Bis-Tris gel, ThermoFisher Scientific). Fluorescence scan was made in a Typhoon FLA 9500 (GE Healthcare LifeSciences) using filters set at 473 nm (excitation wavelength) and 532 nm (emission wavelength). Proteins were transferred to a nitrocellulose membrane (Protan BA85, 0.45  $\mu\text{m}$ , GE Healthcare) at 300 mA for 2.5 h. The membranes were blocked in 5 % milk (skim milk powder, LP0031, Oxiod) in 1x PBS (P1379, Sigma-Aldrich), incubated with a primary antibody diluted in 5 % milk in 0.1 % PBS-Tween 20 (PBST) for 1 h, washed three times for 10 min in 0.1 % PBST, incubated with the secondary antibody diluted in 5 % milk in 0.1 % PBST for 30 min and washed three times again in 0.1 % PBST.  $\beta$ -actin antibody (Sigma-Aldrich, Cat# A5441) was used as a loading control in a 1:10000 dilution for Western blot. IRDye 680LT goat anti-mouse IgG (H+L) (926-68020, Li-COR) were used as a secondary antibody. The signal was detected using direct imaging by the Odyssey Classic imager (Li-Cor).

# Quality analysis of purified reagents

## 1. RhoUb

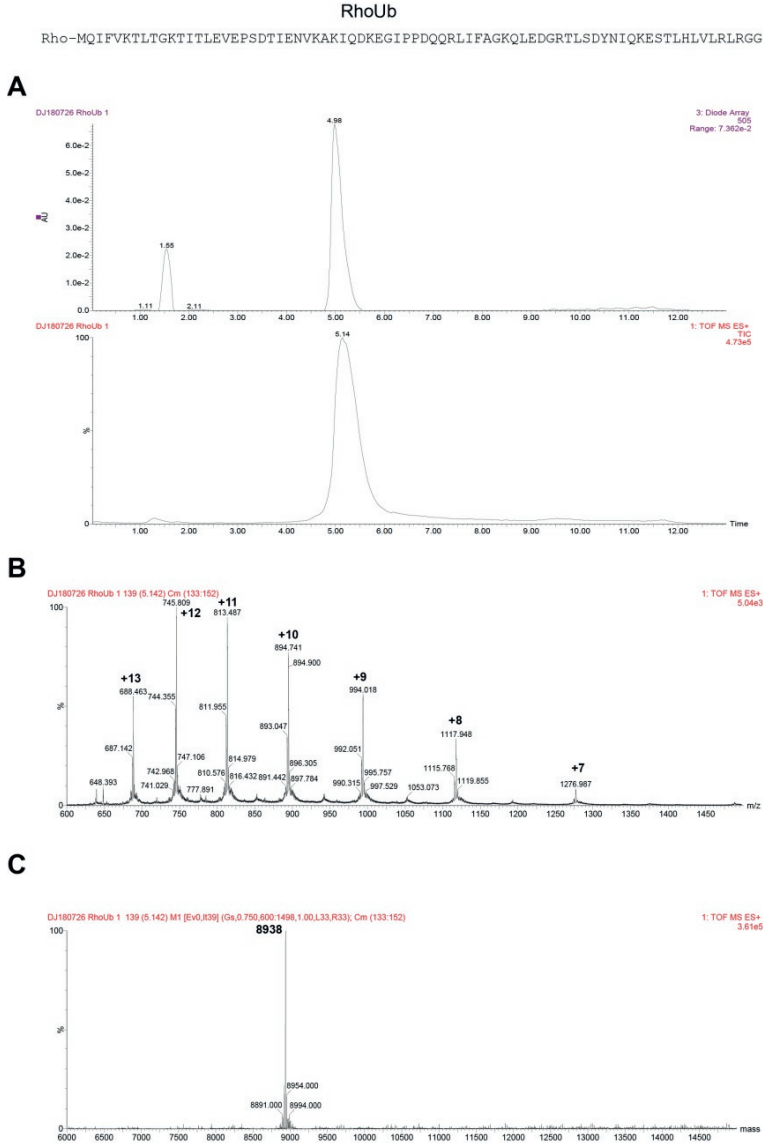
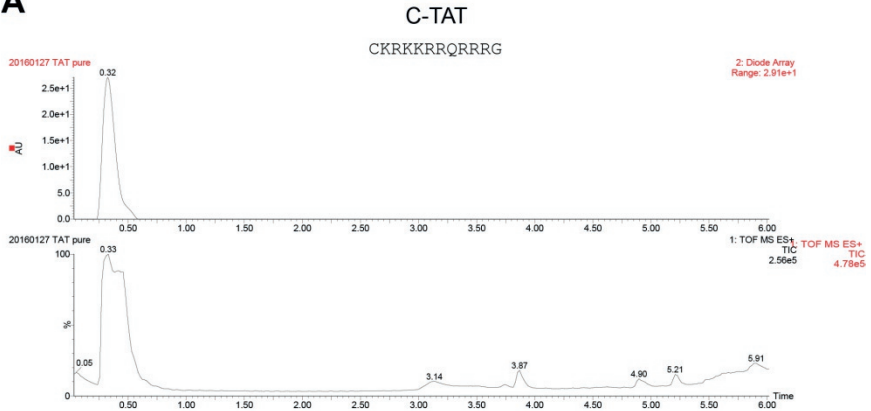


**Figure S5:** RhoUb. **A:** Top: UV chromatogram ( $\lambda$  - 505 nm); Bottom: combined mass spectrum using LC/MS; **B:** Spectrum of the peak at 4.98 min; **C:** Deconvoluted mass of peak spectra. ESI-Mass  $[M+H]$  Calculated: 8940 / Found: 8938.

## 2. C-TAT peptide

A



B

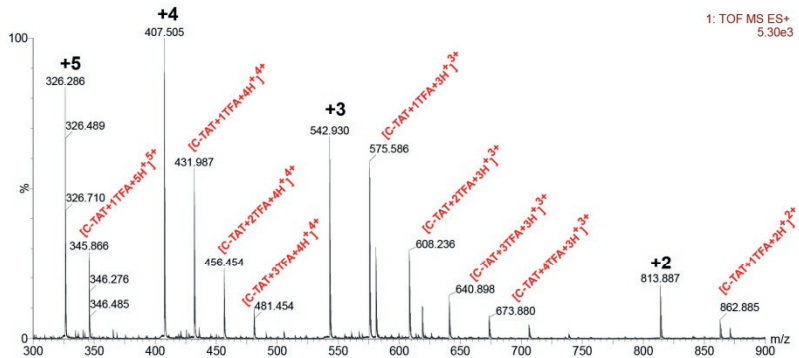


**Figure S6:** C-TAT peptide. **A:** Top: UV chromatogram ( $\lambda$  - 280 nm); Bottom: combined mass spectrum using LC/MS; **B:** Spectrum of the peak at 1.78 min; ESI-Mass  $[M+H]$  Calculated: 1625 / Found:  $[M+4H]^+4+ = 407.33$ ;  $[M+2H]^+2+ = 811.04$ . In addition, 1 to 4 TFA adducts of the C-TAT peptides were also observed as a consequence of using TFA in the peptide-deprotection mix.

### 3. RhoUb-C-TAT

RhoUb-C-TAT

Rho-MQIFVKLTGKTTITLEVPSDTIENVKAKIQDKEGIPPDQQLIFAGKQLEDGRTLSDYNIQKESTLHLVLRGGCKRRKRQRRRG

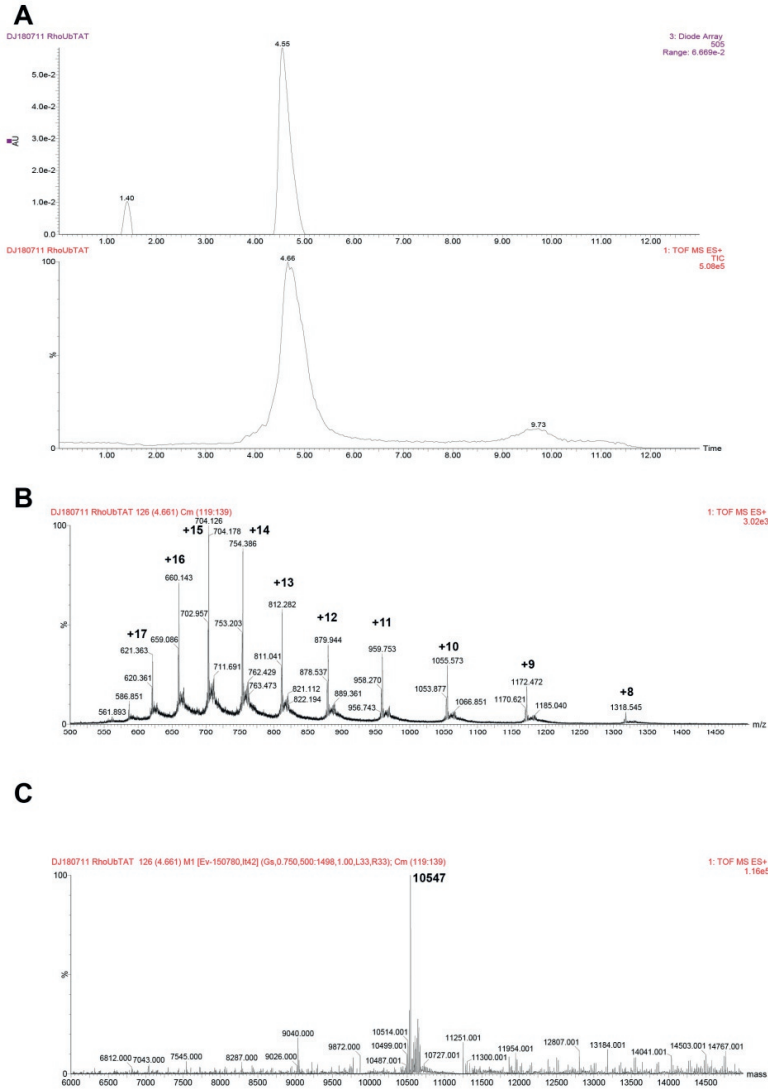


**Figure S7:** RhoUb-C-TAT **A:** Top: UV chromatogram ( $\lambda - 505$  nm); Bottom: combined mass spectrum using LC/MS; **B:** Spectrum of the peak at 4.55 min; **C:** Deconvoluted mass of peak spectra. ESI-Mass  $[M+H]$  Calculated: 10546 / Found: 10547.

4. RhoUb-di-C-TAT

RhoUb-di-C-TAT

Rho-MQIFVKLTGKTITLEVEPSDTIENVKAKIQDKEGIPDPQQLIFAGKQLEDGRTLSDYNIQKESTLHLVLRLLRGCGCKRRKRQRRRG  
 CKRRKRQRRRG

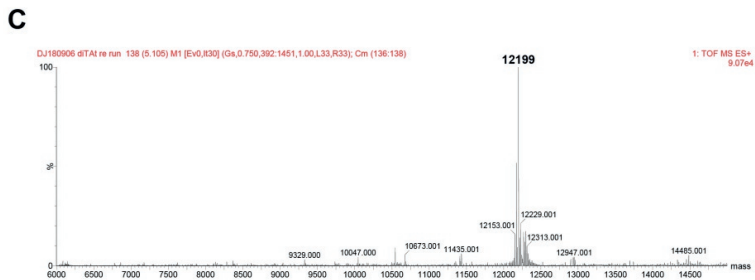
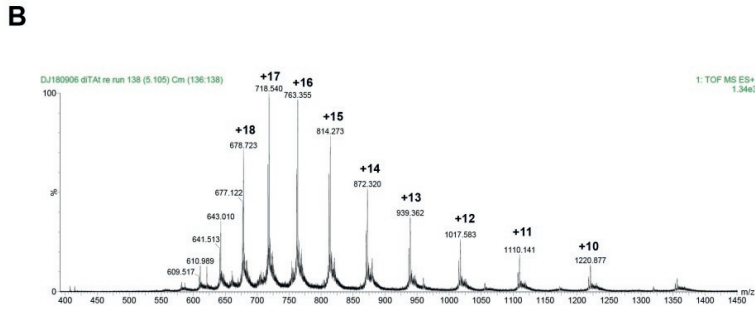
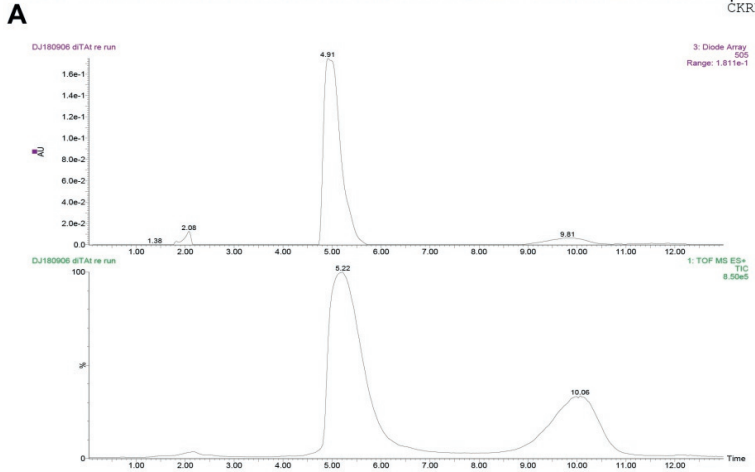


**Figure S8:** RhoUb-di-C-TAT. **A:** Top: UV chromatogram ( $\lambda$  - 505 nm); Bottom: combined mass spectrum using LC/MS; **B:** Spectrum of the peak at 4.62 min; **C:** Deconvoluted mass of peak spectra. ESI-Mass  $[M+H]$  Calculated: 12204 / Found: 12199.

## Supplementary References

1. El Oualid, F., R. Merkx, R. Ekkebus, D.S. Hameed, J.J. Smit, A. de Jong, H. Hilkmann, T.K. Sixma, and H. Ovaa, *Chemical synthesis of ubiquitin, ubiquitin-based probes, and diubiquitin*. *Angew Chem Int Ed Engl*, 2010. **49**(52): p. 10149-53.
2. Geurink, P.P., B.D. van Tol, D. van Dalen, P.J. Brundel, T.E. Mevissen, J.N. Pruneda, P.R. Elliott, G.B. van Tilburg, D. Komander, and H. Ovaa, *Development of Diubiquitin-Based FRET Probes To Quantify Ubiquitin Linkage Specificity of Deubiquitinating Enzymes*. *Chembiochem*, 2016. **17**(9): p. 816-20.
3. Vennegoor, C. and P. Rumke, *Circulating melanoma-associated antigen detected by monoclonal antibody NKI/C-3*. *Cancer Immunol Immunother*, 1986. **23**(2): p. 93-100.